Synthesis and Design of High-Selectivity Wideband Quasi-Elliptic Bandpass Filters Using Multiconductor Transmission Lines

Juan José Sánchez-Martínez, Enrique Márquez-Segura, *Senior Member, IEEE*, and Stepan Lucyszyn, *Fellow, IEEE*

***Abstract*—A comprehensive study of high-selectivity filters that employ series multiconductor transmission lines (MTLs) and a shunt MTL is presented. It is shown that this topology is suitable for implementing three- and five-pole bandpass filters having a quasi-elliptic frequency response. An exact synthesis procedure with analytical design equations for achieving equal-ripple passband response as a function of the operating bandwidth is described. To validate the theory, several bandpass filters are designed, fabricated, and measured. The excellent agreement between the measurements and the predicted results validates the proposed procedure as a reliable and quick technique for designing wideband quasi-elliptic bandpass filters.**

***Index Terms*—Bandpass filter, Butterworth response, Chebyshev response, coupled lines, multiconductor transmission lines (MTLs), quasi-elliptic response, wideband.**

I. Introduction

INCREASING consumer demands for higher data rates and the release of the unlicensed use of the ultra-wideband (UWB) from 3.1 to 10.6 GHz is driving research into new UWB techniques, especially with those having monolithic and hybrid integrated circuit solutions. UWB bandpass filters [1], [2] are key for new applications (in ultrahigh-speed wireless communications and radar systems), where it is necessary to reject undesired signals and to confine transmitted power spectral densities. Several imperfections and impairments occur in the RF components that, if not corrected for, can cause spectrum regrowth, interference, and noise, degrading the performance of the system. Thus, it is important to realize filters with sharp cut-off regions, low insertion losses, low in-band group-delay variation, and flat amplitude responses.

Consequently, in recent years, there has been growing interest in the design of bandpass filters with large fractional bandwidths and high selectivity. Conventional microwave filter theory is based on narrowband fractional bandwidths [3], [4], which has prompted the development of new types of broadband filters [1], [2], [5]. A variety of filters have been reported, with different forms of multiple-mode-resonator (MMR) having stepped-impedance or stub-loaded configurations, in order to position the first resonant frequencies into the desired wide passband [6]–[26]. Most of these MMR-based filters combine parallel-coupled lines with different types of MMR structures.

The conventional high-pass prototype with short-circuited stubs for designing wideband bandpass filters have been explored in [27] and [28]. Bandpass filters with single and multiple stages using composite series and shunt stubs are proposed in [11], and ring-based wideband bandpass filters are described in [29], [30]. Wideband filters based on transversal signal-interaction concepts have been realized in [31], and a stepped-impedance parallel-coupled microstrip structure is employed in [32]. Nevertheless, although a great amount of wideband bandpass filters have been reported, in most of these works, there lacks a systematic design methodology, based purely on filter synthesis (i.e., without the need for additional tuning or optimization to reach the final specifications). Only few works, as in [8]–[13], [30], [33], and [34], face this issue in order to calculate the circuit design parameters for achieving a specific frequency response.

A shunt-coupled $\lambda/4$ short-circuited line section was used in [17] to design bandpass filters with two transmission zeros. According to the study presented in [17], only a three-pole bandpass filter can be designed by using $\lambda/4$ open input/output coupled lines. Therefore, the two $\lambda/4$ open-circuited lines are replaced by two $\lambda/2$ short-circuited lines to generate two additional transmission poles within the pass band. However, here it is demonstrated that, with two input and output $\lambda/4$ coupled-line sections, it is possible to design both three- and five-pole filters. Moreover, closed-form design equations are provided for both conditions.

The use of two and three shunt-coupled lines to design wideband bandpass filters was previously addressed in [19], but only equations for the special two-strip case were given and without design guidelines. More recently, a shunt broad-side-coupled microstrip/CPW stub was used in [20] to generate two transmission zeros, improving the upper passband selectivity. However, although some equations were given to calculate the resonance frequencies of the structure, there was no design procedure neither for the input/output coupled lines or for the shunt structure, to obtain a desired frequency response.

Manuscript received April 07, 2014; revised September 16, 2014; accepted November 15, 2014. Date of publication December 18, 2014; date of current version December 31, 2014.

J. J. Sánchez-Martínez and E. Márquez-Segura are with the Departamento de Ingeniería de Comunicaciones, Escuela Técnica Superior de Ingeniería de Telecomunicación, Universidad de Málaga, 29071 Málaga, Spain (e-mail: jjsm@ic.uma.es; ems@ic.uma.es).

S. Lucyszyn is with the Department of Electrical and Electronic Engineering, Imperial College London, London SW7 2AZ, U.K. (e-mail: s.lucyszyn@imperial.ac.uk).

Color versions of one or more of the figures in this paper are available online at http://ieeexplore.ieee.org.

Digital Object Identifier 10.1109/TMTT.2014.2375323

In [26], authors presented the analysis of a compact filtering structure consisting of one series and one shunt wire-bonded multiconductor transmission lines (MTLs). This compact structure allows the design of bandpass filters to have a high-selectivity quasi-elliptic function response, which can only be achieved with three transmission poles. Moreover, it is difficult to obtain higher rejection levels while also having good return losses.

In this work, a wideband planar bandpass filter consists of two series MTL and a shunt short-circuited MTL is analyzed in rigorous detail and a comprehensive study of the filter is presented for the first time. By using the proposed topology and design techniques, three- or five-pole wideband bandpass filters having two transmission zeros on both sides of the passband can be easily designed. A set of accurate analytical design equations are derived from first principles, which allows the designer to optimize the in-band flatness and enhance the roll-off slopes at the cutoff frequencies. The new topology can enhance the filter's performances for the asymmetric structure that we recently introduced in [26], and the new synthesis methodology allows for a greater degree of control over the desired frequency response.

This paper is structured as follows. First, to provide some insights into the physical behavior of the filter, both series and shunt wire-bonded MTLs are analyzed separately in Sections II-A and II-B, respectively. Some preliminary design equations are obtained to clarify the effects and benefits of introducing the shunt MTL. Based on this theory, the whole structure is rigorously analyzed in Section II-C. A complete set of analytical design equations are derived and a design methodology is given to obtain the desired frequency response. How the shunt short-circuited wire-bonded MTL is used, not only for generating two transmission zeros but also to include two new transmission poles within the passband, is described. Finally, in Section III, a number of filters are designed, fabricated, and measured to validate our new theory and techniques.

II. Theoretical Analysis

The transmission-line equivalent circuit model for the proposed wideband bandpass filter is given in Fig. 1. The T-structure filter consists of two series input–output wire-bonded MTLs and a shunt short-circuited wire-bonded MTL. The wire-bonded MTL is a specific case of multiconductor transmission lines, in which bonding wires interconnect the ends of alternate conductors. Assuming ideal short circuits across alternate conductors (i.e., the bonding wires are very short compared to wavelength and have insignificant series inductor or resistance), the connections can be neglected and the equivalent circuit model for a wire-bonded MTL can be reduced to just a pair of coupled lines [35]. As a result, with this simplified configuration, there are now only two independent conductors and the operating bandwidth is increased, since undesired resonances are suppressed. This scenario allows the use of a simplified model in order to obtain analytical design equations [36]. The use of wire-bonded MTLs is recommended for achieving tight coupling, which would not be possible with only two strips without any backside aperture [35].

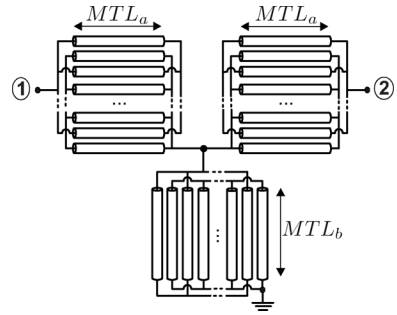

Fig. 1. Transmission-line equivalent circuit model for the proposed wideband bandpass filter consisting of two series and one shunt wire-bonded MTLs.

In the following equations, subscripts a and b represent the series and shunt wire-bonded MTLs, respectively (as also seen in Fig. 1). However, for common expressions, the variable i is also used; this can represent either a or b.

A. Analysis of Two Series Wire-Bonded MTLs

The layout of a two-port wire-bonded MTL in microstrip technology is shown in Fig. 2(a). This element was used in [37] to design a broadband balun, and a transmission-line equivalent circuit model was obtained in [38], as a function of the number of strips. Assuming a lossless medium, its admittance matrix can be given as

$$[Y]_a = \frac{(M_a^2 - N_a^2)\sin\theta_a}{M_a^2\cos^2\theta_a - N_a^2}\begin{bmatrix} jM_a\cos\theta_a & jN_a \\ jN_a & jM_a\cos\theta_a \end{bmatrix} \quad (1)$$

where M_a and N_a are related to the even- and odd-mode impedances of a pair of coupled lines [39]

$$M_i = \frac{1}{Z_{oe_i} + Z_{oo_i}}\left(1 + \frac{(k_i - 1)}{2}\frac{Z_{oe_i}^2 + Z_{oo_i}^2}{Z_{oe_i}Z_{oo_i}}\right) \quad (2a)$$

$$N_i = \frac{k_i - 1}{2}\frac{Z_{oo_i} - Z_{oe_i}}{Z_{oe_i}Z_{oo_i}} \quad (2b)$$

where k_i represents the number of conductors and θ_a is the electrical length of the conductors, which is calculated as the average value for the even- and odd-mode electrical lengths (an approximation for inhomogeneous substrates) [35], [36], [40]. From (1), the image impedance of the series wire-bonded MTL can be expressed as

$$Z_{I_a} = Z_{0_a}\sqrt{1 + \left(1 - \frac{1}{c_a^2}\right)\cot^2\theta_a} \quad (3)$$

with

$$Z_{0_a} = \frac{-N_a}{M_a^2 - N_a^2} \quad (4)$$

and c_a is equal to the maximum coupling coefficient of a k-line quarter-wavelength four-port coupler, given by [39]

$$c_i = \frac{-N_i}{M_i}. \quad (5)$$

The image impedance can be used to design the input–output coupled-line structures [3] and it is of great importance for understanding the behavior of the two-port wire-bonded MTL.

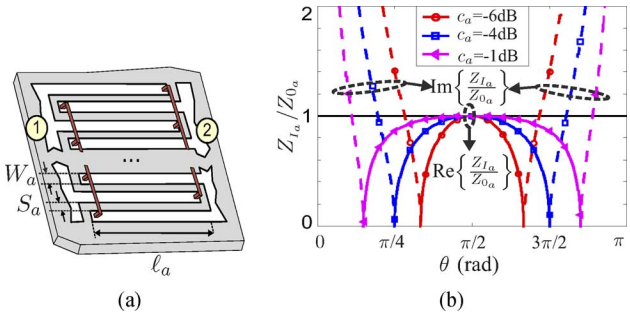

(a) (b)

Fig. 2. (a) Layout and (b) image impedance of a two-port wire-bonded MTL.

Fig. 2(b) represents the image impedance (3) normalized by Z_{0_a} for several coupling factors c_a. As seen, Z_{0_a} is the image impedance value of the structure at $\theta_a = \pi/2$, that normally corresponds to the design center frequency. There is a frequency range where the image impedance is purely real, which can be broadened by increasing the coupling factor. However, outside of this frequency range, the image impedance is purely imaginary and the MTL behaves as an inductive reactance. From these curves it is straightforward to deduce that if the MTL is a quarter-wavelength long at the design center frequency, and with Z_0 being the reference impedance at both ports, the wire-bonded MTL can be designed to be perfectly matched at one (with $Z_{0_a} = Z_0$) or two frequencies (with $Z_{0_a} > Z_0$). Therefore, a single-section wire-bonded MTL can be easily designed to have either a Butterworth or a Chebyshev response, having two transmission poles [41].

However, the proposed topology includes two cascaded wire-bonded MTLs, and, for this configuration, the design procedure using the insertion loss method is preferred over the use of the image impedance, in order to synthesize the desired frequency response. The insertion loss method allows a higher degree of control over the passband and stopband characteristics. By using the admittance matrix in (1), the square of the magnitude of S-parameters for two-stage wire-bonded MTLs reduce to

$$|S_{11_s}|^2 = \frac{F_s^2}{1+F_s^2} \quad |S_{21_s}|^2 = \frac{1}{1+F_s^2} \tag{6}$$

with

$$F_s = \frac{c_a^2 - \bar{Z}_{0_a}^2}{\bar{Z}_{0_a} c_a^3} \frac{\cos\theta}{\sin\theta} \left(\cos^2\theta + \frac{c_a^2\left(\bar{Z}_{0_a}^2 - 1\right)}{c_a^2 - \bar{Z}_{0_a}^2} \right) \tag{7}$$

where subscript s is used to denote this configuration with two series MTL and $\bar{Z}_{0_a}$ is the normalized impedance of the MTL (with Z_{0_a}/Z_0). From the transfer function (6) and with (7), it is possible to derive analytical design equations to obtain either a Butterworth or Chebyshev type response, but having three transmission poles. The design equations can be calculated by setting $Z_{0_a} = Z_0$, if a Butterworth response is desired, or by equating F_s with a standard third order Chebyshev polynomial for a Chebyshev response. For a bandpass filter, the fractional bandwidth (FBW) is defined as

$$\text{FBW} = \frac{f_{c2} - f_{c1}}{f_o} \tag{8}$$

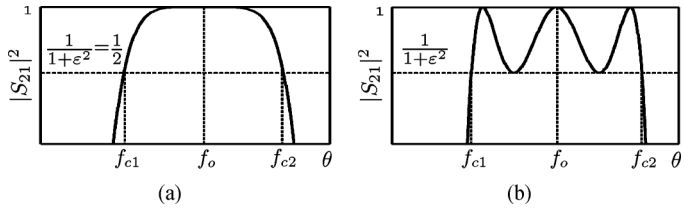

(a) (b)

Fig. 3. (a) Butterworth and (b) Chebyshev passband responses using (10).

where f_o is the design frequency and f_{c1} and f_{c2} are the passband limits of the filter (Fig. 3). In addition, by considering that the MTLs are one-quarter wavelength at the design frequency and assuming a TEM propagation, it is possible to obtain the electrical length of the structure at the lower cutoff frequency f_{c1} as

$$\theta_{c1} = \theta_o \left(1 - \frac{\text{FBW}}{2}\right) = \frac{\pi}{2}\left(1 - \frac{\text{FBW}}{2}\right). \tag{9}$$

Fig. 3 shows typical maximally flat and equal-ripple responses. With the latter, for the Chebyshev filter, the passband limits are established for the equal ripple-level. Here, ε is a ripple constant related to a given return loss L_R in decibels within the pass band, given by the common textbook expression [1]

$$\varepsilon = \frac{1}{\sqrt{10^{L_R/10} - 1}}. \tag{10}$$

In contrast, for the Butterworth filter, f_{c1} and f_{c2} are the -3-dB points of the frequency response; thus, the return loss $L_R = 3$ dB and, consequently, $\varepsilon = 1$.

Taking into account the above-mentioned considerations and by analyzing (6) and (7), the following closed-form analytical design equations are found to synthesize wideband bandpass Butterworth and Chebyshev filters.

1) Third-Order Butterworth Response: From (6), if $Z_{0_a} = Z_0$, a maximally flat (i.e., Butterworth) response is obtained. The associated design equations to obtained the desired operating bandwidth are

$$c_a = S_1 + S_2 - \frac{1}{3G} \tag{11}$$

where

$$G = \varepsilon \tan\theta_{c1}\left(1 + \tan^2\theta_{c1}\right) \tag{12a}$$

$$R = \frac{1}{2G} - \frac{1}{27G^3}$$

$$Q = -\frac{1}{9G^2} \tag{12b}$$

$$S_1 = \sqrt[3]{R + \sqrt{Q^3 + R^2}}$$

$$S_2 = \sqrt[3]{R - \sqrt{Q^3 + R^2}}. \tag{12c}$$

This solution is exact and allows the value of c_a to be calculated as a function of the fractional bandwidth (9). If the FBW is defined for a return losses of $L_R = 3$ dB, then $\varepsilon = 1$.

2) Third-Order Chebyshev Response: For a Chebyshev filter, the design equations are created by comparing F_s of (7) with

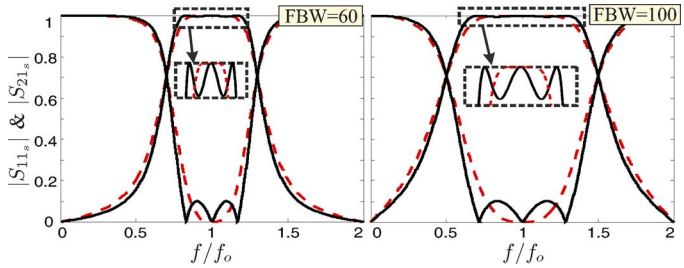

Fig. 4. Calculated magnitudes of S_{11} and S_{21} for two-stage wire-bonded MTL filters designed with Butterworth (dashed line) and Chebyshev (solid line) responses for two 3-dB FBWs of 60% and 100%.

a third-order Chebyshev polynomial [3]. As a result, the following design equations as a function of the fractional bandwidth and ripple level are found [42]:

$$c_a = \sqrt{\frac{\cos^3\theta_{c1}(u^2-1)}{4u\varepsilon}} \tag{13a}$$

$$\bar{Z}_{0_a} = \sqrt{1+\frac{3}{4}(u^2-1)\cos^2\theta_{c1}} \tag{13b}$$

where u is given by

$$u = S_1 + S_2 + \frac{\varepsilon}{\cos\theta_{c1}} \tag{14}$$

with

$$S_1 = \sqrt[3]{r+g}$$
$$S_2 = \sqrt[3]{r-g} \tag{15a}$$

$$r = \frac{\varepsilon\left(\varepsilon^2 - \cos^2\theta_{c1} + 2\right)}{\cos^3\theta_{c1}} \tag{15b}$$

$$g = \sqrt{\frac{3\varepsilon^2\left(6\cos^4\theta_{c1} - (27\varepsilon^2+36)\cos^2\theta_{c1} + 36(1+\varepsilon^2)\right) - \cos^6\theta_{c1}}{27\cos^6\theta_{c1}}}. \tag{15c}$$

It is important to emphasize that, because of the $\sin\theta$ term in the denominator of F_s, F_s is not a standard Chebyshev polynomial, and, thus, the obtained design (13) will provide an approximated synthesis procedure. Nevertheless, this fact can be dealt with (as in [25]), but it involves the use of laborious expressions and, in general, approximated solutions are more suitable. After obtaining the design values of Z_{c_a} and c_a for a particular operating bandwidth, they can be easily corrected for by means of (6) to compensate for the effect of $\sin\theta$.

Using (11) and (13), two Butterworth and Chebyshev filters are designed for two 3-dB FBWs of 60% and 100%. The Chebyshev filter is designed for a return loss L_R of 20 dB, and its equal-ripple bandpass is adjusted to meet the 3-dB FBW. The computed design values of these filters are shown in Table I, and the magnitudes of their calculated S-parameters are given in Fig. 4. As expected, by using the Chebyshev type, both the selectivity of the filter and in-band flatness are improved. Therefore, the closed-form expressions (11) and (13) provide a quick design procedure for Butterworth and Chebyshev filters, having a specific bandwidth and in-band flatness. To achieve sharpened roll-off skirts, in the next subsection, a shunt wire-bonded MTL will be used to place two transmission zeros at the lower and upper cutoff frequencies.

TABLE I
DESIGN PARAMETERS OF TWO BUTTERWORTH AND CHEBYSHEV FILTERS

	Butterworth		Chebyshev (LR=20dB)		
FBW_{3dB} (%)	c_a (dB)	Z_{0_a} (Ω)	c_a (dB)	Z_{0_a} (Ω)	FBW^* (%)
60	-7.15	50	-7.48	61.6	39.25
100	-3.65	50	-3.78	60.7	66.7

FBW^*: Fractional bandwidth with equal-ripple response

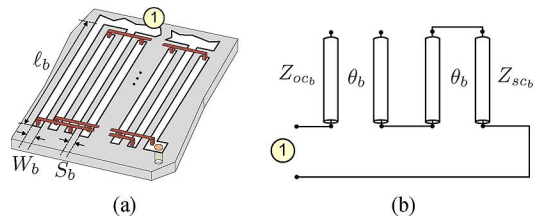

Fig. 5. (a) Layout and (b) equivalent circuit model for the shunt short-circuited wire-bonded MTL.

B. Analysis of the Shunt Short-Circuited Wire-Bonded MTL

The shunt section used in the proposed filter is created by short-circuiting the output port of a two-port wire-bonded MTL [i.e., port 2 in Fig. 2(a)]. The layout and equivalent circuit model for this one-port circuit are given in Fig. 5. This element, which was previously analyzed in [43], is equivalent to a pair of series short-circuited and open-circuited shunt stubs, having equivalent characteristic impedances Z_{oc_b} and Z_{sc_b} given by

$$Z_{oc_b} = Z_{0_b}\frac{1-c_b^2}{c_b}, \quad Z_{sc_b} = Z_{0_b}\,c_b \tag{16}$$

with (4) and

$$Z_{0_b} = \frac{-N_b}{M_b^2 - N_b^2}. \tag{17}$$

The input admittance Y of the shunt section can be easily calculated from

$$Y = \frac{1}{Z_{in_b}} = j\frac{1}{Z_{0_b}}\left(\frac{1-c_b^2}{c_b}\cot\theta_b - c_b\tan\theta_b\right)^{-1} \tag{18}$$

where c_b is the coupling coefficient, as defined in (5). The imaginary part of Y, normalized by $Y_{0_b} = 1/Z_{0_b}$, is represented in Fig. 6 for several coupling levels. As can be seen, the structure has two poles and three zeros. The zeros always appear at $\theta_b = 0, \pi/2$ and π, regardless of the value of c_b, but the position of the poles can be controlled by simply adjusting the value of c_b. Taking into account this frequency response, the shunt MTL can be used as a shunt resonator, to create transmission zeros at different electrical lengths. These electrical lengths can be calculated as [43]

$$\theta_{pn} = \pm\theta_{p0} + n\pi \tag{19}$$

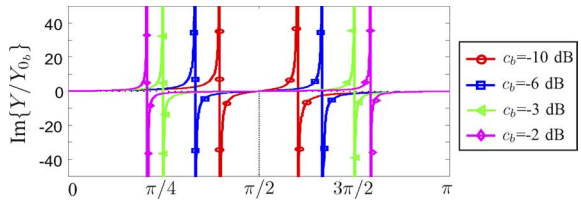

Fig. 6. Input admittance of the shunt short-circuited MTL for several coupling c_b values.

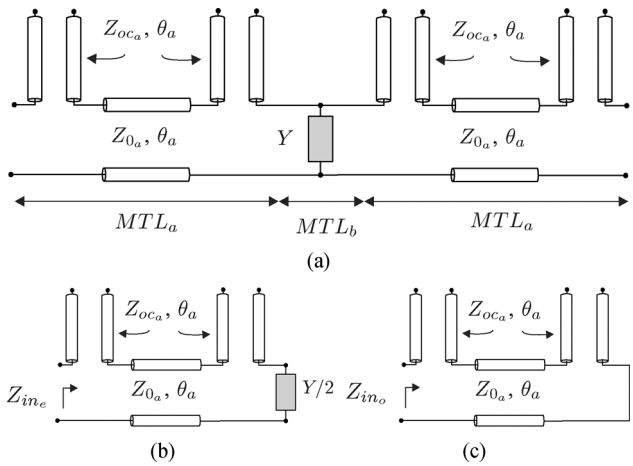

Fig. 7. (a) Equivalent circuit model for the proposed filter and corresponding circuits under (b) even- and (c) odd-mode excitations.

where

$$\theta_{p0} = \arccos\left(\frac{|N_b|}{M_b}\right) = \arccos\left(c_b\right) \tag{20}$$

and $n = 0, 1, 2, 3, \ldots$. Consequently, from Fig. 6 it can be deduced that the shunt structure is appropriate for inserting two transmission zeros at the cutoff frequencies (θ_{p0} and $\pi - \theta_{p0}$) of the bandpass filter. As it will be shown in the next section, the shunt short-circuited wire-bonded MTL will be designed not only to generate two transmission zeros but also to include two new transmission poles within the passband.

C. Analysis for the Complete Filter

The equivalent circuit transmission-line model for the proposed filter, comprising of two series wire-bonded MTLs and a shunt short-circuited wire-bonded MTL, is depicted in Fig. 7(a). The shunt MTL is modeled as a shunt admittance Y (18), while the open-circuited MTL is represented by its equivalent circuit consisting of a transmission-line section with two series open circuit stubs [38]. Z_{0_a} was defined in (4) and Z_{oc_a} is given by

$$Z_{oc_a} = Z_{0_a}\frac{1 - c_a}{c_a}. \tag{21}$$

From Fig. 7(a), it can be seen that the configuration of the proposed filter is a symmetrical structure and thus, the analytical study of this arrangement can be easily decomposed into even- and odd-mode excitations, as shown in Fig. 7(b) and (c), respectively. To achieve the maximum operating bandwidth, both series and shunt wire-bonded MTLs are designed with a length of $\lambda/4$ at the design center frequency f_o. Therefore, it can be considered that their electrical lengths θ_a and θ_b are similar and equal to $\theta = (\pi/2)(f/f_o)$, and the even- and odd-mode input impedances can be expressed as

$$Z_{\text{in}_e} = jZ_{0_a}\frac{\left(Z_{0_a}c_a + 2Z_{0_b}c_b\right)\tan^2\theta - \left(\frac{1-c_a^2}{c_a}Z_{0_a} + 2Z_{0_b}\frac{1-c_b^2}{c_b}\right)}{c_a\left(\left(\frac{Z_{0_a}}{c_a} - 2Z_{0_b}\frac{1-c_b^2}{c_b}\right)\tan\theta - 2Z_{0_b}c_b\tan^3\theta\right)} \tag{22a}$$

$$Z_{in_o} = -jZ_{0_a}\left(\frac{1-c_a^2}{c_a}\cot\theta - c_a\tan\theta\right). \tag{22b}$$

Using the definitions (22a) and (22b), the S-parameters of the proposed structure are easily determined in terms of Z_{in_e} and Z_{in_o} as

$$S_{11} = \frac{Z_{\text{in}_e}Z_{\text{in}_o} - Z_0^2}{\Delta}$$
$$S_{21} = \frac{Z_0\left(Z_{\text{in}_e} - Z_{\text{in}_o}\right)}{\Delta} \tag{23a}$$
$$\Delta = Z_0^2 + Z_0\left(Z_{in_e} + Z_{\text{in}_o}\right) + Z_{\text{in}_e}Z_{\text{in}_o} \tag{23b}$$

where Z_0 is the characteristic impedance used to terminate the input and output ports. By evaluating (23) and after several algebraic manipulations and rigorous transformations, the squared magnitude of S_{11} and S_{21}, are of the same form as (6)

$$|S_{11}|^2 = \frac{F^2}{1+F^2}, \quad |S_{21}|^2 = \frac{1}{1+F^2} \tag{24}$$

but with

$$F = \left(\frac{c_b}{2c_a^4\bar{Z}_{0_b}}\right)\frac{\cos\theta\left(g_4\cos^4\theta + g_2\cos^2\theta + g0\right)}{\left(c_b^2 - \cos^2\theta\right)\sin\theta} \tag{25a}$$

$$g_4 = \left(\bar{Z}_{0_a}^2 - c_a^2\right)\left(\frac{2c_a\bar{Z}_{0_b}}{c_b\bar{Z}_{0_a}} + 1\right) \tag{25b}$$

$$g_2 = \frac{2c_a\bar{Z}_{0_b}}{c_b\bar{Z}_{0_a}}\left(c_a^2\left(1+c_b^2\right) - \bar{Z}_{0_a}^2\left(c_a^2+c_b^2\right)\right) + c_a^2\left(1-2\bar{Z}_{0_a}^2\right) \tag{25c}$$

$$g_0 = c_a^3\left(\bar{Z}_{0_a}^2c_a + 2\frac{\bar{Z}_{0_b}}{\bar{Z}_{0_a}}c_b\left(\bar{Z}_{0_a}^2 - 1\right)\right) \tag{25d}$$

$$\bar{Z}_{0_a} = \frac{Z_{0_a}}{Z_0}$$
$$\bar{Z}_{0_b} = \frac{Z_{0_b}}{Z_0}. \tag{26}$$

The form of F (25a) shows that the proposed topology is straightforward for the design of selective bandpass filters having a quasi-elliptic response. The rational function F has simple poles at $\cos\theta = c_b$ and its numerator is a fifth-order polynomial. This topology is also suitable for the design of a five-pole passband filter with two transmission zeros [1], [44]. This result highlights the main difference between the proposed symmetric topology and the asymmetric configuration presented in [26]. In [26], a compact filtering structure was analyzed to obtain a three-pole bandpass filter. However, by including the output series MTL, two new poles can be created that improve both the flatness and the selectivity of the

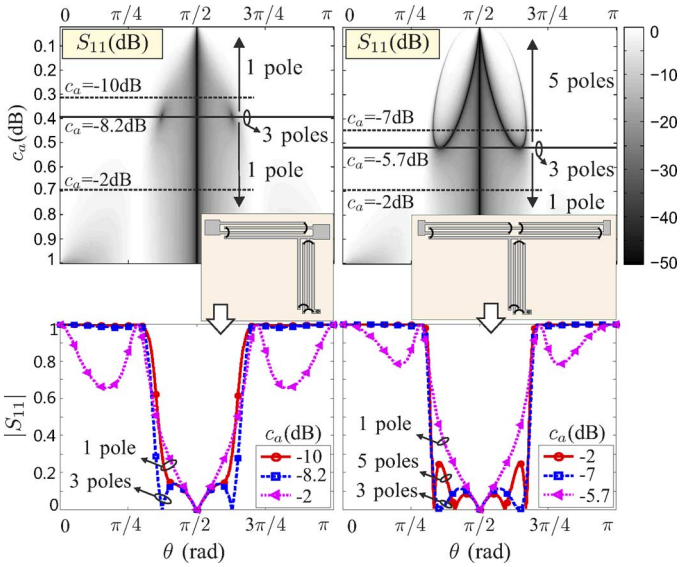

Fig. 8. Magnitude of S_{11} as a function of c_a considering an asymmetric or symmetric filtering topology. $\bar{Z}_{0_a} = \bar{Z}_{0_b} = 1$, $c_b = -4$ dB.

passband. Fig. 8 shows the contour plots for the magnitude of S_{11} for the asymmetric and symmetric topologies, as a function of c_a, for a particular value of $\bar{Z}_{0_a} = \bar{Z}_{0_b} = 1$ and $c_b = -4$ dB. From these curves, it can now be seen that the asymmetric scheme can only be designed to have three transmission poles, while the symmetric filter can be configured to have three or five poles. Moreover, where the asymmetric filter has three poles the range of values for c_a is very small. In contrast, for the symmetric configuration, there is a coupling level c_a where the filter presents three transmission poles and, for lower values the filter always has five poles. This frequency behavior demonstrates that the new topology not only provides a better frequency response but is also less sensitive to small deviations from the theoretical design parameters.

The design of the proposed filter for an equal-ripple pass band can be directly accomplished by evaluating (24). However, its frequency response depends on c_a, Z_{0_a}, c_b and Z_{0_b}, and this involves a laborious process in order to achieve the desired bandwidth with particular insertion losses or rejection level and with an equal-ripple passband. Therefore, analytical equations are desirable for a quick design process. This procedure is carried out by comparison of F with the rational function $f(x)$ [44] as

$$f(x) = \frac{\alpha^2 x T_{n-1}(x) + \beta^2 x T_{n-3}(x) - 2a^2 T_{n-2}(x)}{2\,(a^2 - x^2)} \tag{27a}$$

$$\alpha = a + \sqrt{a^2 - 1}$$
$$\beta = a - \sqrt{a^2 - 1} \tag{27b}$$

where $f(x)$ is expressed in terms of Chebyshev polynomials of order n. This has simple poles at $x = \pm a$, and the equal-ripple passband is determined for $-1 \leq \mathrm{x} \leq 1$. This region is mapped to the passband of the filter by replacing $\cos\theta$ with $\cos\theta / \cos\theta_{c1}$ to map $x = 1$ to θ_{c1}. After this substitution, a can be written as

$$a = \frac{\cos\theta_{p0}}{\cos\theta_{c1}} = \frac{c_b}{\cos\theta_{c1}} \tag{28}$$

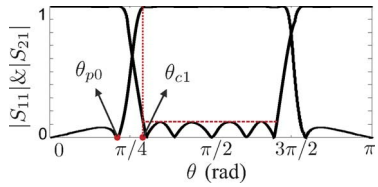

Fig. 9. Magnitude of S-parameters for a quasi-elliptic filter having five transmission poles and two transmission zeros.

which defines the ratio between the transmission zero θ_{p0} and the cutoff frequency θ_{c1}, where $a > 1$, as illustrated in Fig. 9. The lower the value of a, the closer the transmission zeros are to the cut-off frequencies. From (28), it is seen that for a particular FBW, c_b is determined for each value of a.

In addition, from (24) and (27), the following relationships between the design parameters are found to design a five-pole quasi-elliptic filter:

$$\bar{Z}_{0_a} = \left(\frac{-C_2 - \sqrt{C_2^2 - 4C_4C_0}}{2C_4} \right)^{1/2} \tag{29a}$$

$$\bar{Z}_{0_b} = \frac{c_a c_b \bar{Z}_{0_a} [\bar{Z}_{0_a}^2 (Ac_a^2 + 2B) - B]}{2[c_a^2(B + c_b^2(A + B)) - \bar{Z}_{0_a}^2 (c_a^2(B + Ac_b^2) + Bc_b^2)]} \tag{29b}$$

where

$$A = \frac{2(\beta^2 - 4\alpha^2 - 4a^2)\cos\theta_{c1}^2}{8\alpha^2}$$
$$B = \frac{(6a^2 + \alpha^2 - \beta^2)\cos\theta_{c1}^4}{8\alpha^2} \tag{30a}$$

$$C_0 = c_a^4 c_b^2 \,(1 + A + B) \tag{30b}$$

$$C_2 = c_a^6(A + 1 + c_b^2) + c_a^4(B - c_b^2(3 + A)) - c_a^2 c_b^2 (A + 2B) \tag{30c}$$

$$C_4 = Bc_b^2 - c_a^6 + c_a^4(c_b^2 - A) + c_a^2(Ac_b^2 - B). \tag{30d}$$

Equation (29) can be easily solved and allows the characteristic impedances of the series and shunt MTL ($\bar{Z}_{0_a}$ and $\bar{Z}_{0_b}$) to be calculated as a function of c_a and c_b in order to obtain a particular equal-ripple operating bandwidth. The solutions of the above equations guarantee that the designed filter will have a quasi-elliptic response with five transmission poles and two transmission zeros. The design procedure can be summarized as follows.

Step 1) Calculate θ_{c1} according to the desired operating bandwidth with equiripple response (9) (see Fig. 9).

Step 2) Specify a particular value of a, taking into account the required selectivity. The lower the value of a the closer the attenuation poles to the cutoff frequency and, consequently, the greater the skirt selectivity of the filter. Once the value of a is determined, c_b is computed as $c_b = a\cos\theta_{c1}$ in (28).

Step 3) Obtain values for $\bar{Z}_{0_a}$ and $\bar{Z}_{0_b}$, as a function of c_a, using (29).

Step 4) Evaluate (25a) with the computed values c_b, c_a, $\bar{Z}_{0_a}$ and $\bar{Z}_{0_b}$, to obtain the desired minimum return losses (or ripple level) and the minimum stopband rejection level.

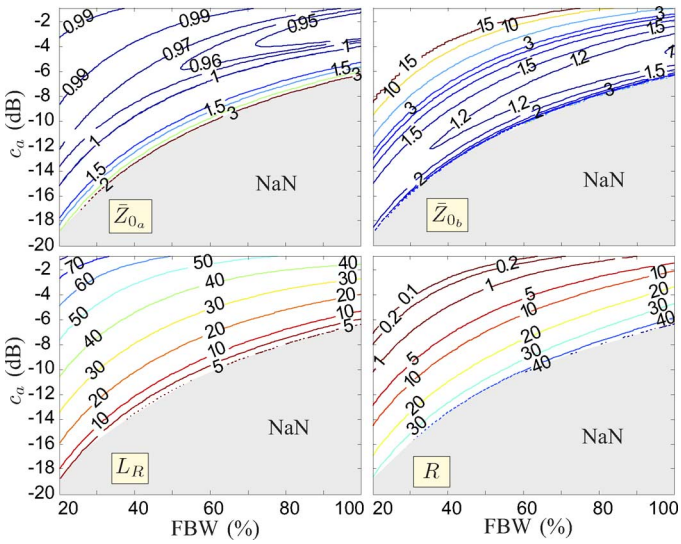

Fig. 10. Design parameters $\bar{Z}_{0_a}$ and $\bar{Z}_{0_b}$, return loss L_R (dB) and minimum out-of-band rejection level R (dB) as a function of both, the coupling factor c_a of the series MTL and the fractional equal-ripple bandwidth FBW.

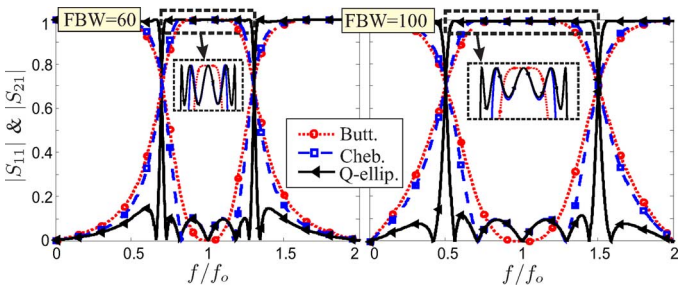

Fig. 11. Magnitude of S_{11} and S_{21} for a two-stage wire-bonded MTL filter designed with a Butterworth and Chebyshev response, and the proposed quasi-elliptic filter for two 3-dB FBWs of 60% and 100%.

Step 5) Select the values of c_a, $\bar{Z}_{0_a}$ and $\bar{Z}_{0_a}$ to obtain a particular rejection level and ripple value. If a higher rejection level is needed, increase the value of a and go back to step 2). By increasing a, the skirt selectivity is reduced but the minimum rejection level is improved.

Using the above design procedure, Fig. 10 shows the contour plots for the design parameters obtained as a function of the fractional bandwidth, for a particular value of $a = 1.2$. It can be seen that, depending on the final selected values, it is possible to change both the return losses and the minimum rejection level. Furthermore, for a particular FBW, the lower the return losses (higher ripple level) the higher the rejection level. Therefore, to improve the out-band rejection without reducing the return losses, it is necessary to use a higher value of a (decreasing the skirt selectivity). However, it is important to mention that the allowed values of Z_{0_a}, c_a, Z_{0_b} and c_b will be dictated by the fabrication process.

To highlight the enhancement of the filtering performances by including the shunt MTL, Fig. 11 shows the S-parameters for

TABLE II
DESIGN PARAMETERS FOR A FIVE-POLE QUASI-ELLIPTIC FILTER

	Quasi-elliptic (LR=20dB, a=1.2)				
FBW_{3dB} (%)	c_a (dB)	Z_{0_a} (Ω)	c_b (dB)	Z_{0_b} (Ω)	FBW^* (%)
60	-7.5	51	-5.8	61.2	56
100	-4.4	50	-2	52.4	92

FBW^*: Fractional bandwidth with equal-ripple response

Butterworth and Chebyshev filters, with only two series MTLs, and of the proposed quasi-elliptic filter for two 3-dB fractional operating bandwidths of 60% and 100% ($L_R = 20$ dB for Chebyshev and quasi-elliptic responses). The improvements in the skirt selectivity and flatness of the pass band are exceptionally good. The design parameters are given in Table II, and, compared with Table I, it is seen that, for both 3-dB operating bandwidths, the FBW with the equal-ripple response is increased by approximately 40%.

The general design equations in (29) can be greatly simplified if $\bar{Z}_{0_a} = 1$ (i.e., $Z_{0_a} = Z_0$). Under this specific condition, the following two closed-form design equations are found:

$$c_a = \left(\frac{-B(1+c_b^2) + \sqrt{B^2(1+c_b^2)^2 + 4Bc_b^2(A+c_b^2)}}{2(A+c_b^2)} \right)^{1/2} \tag{31a}$$

$$\bar{Z}_{0_b} = \frac{c_a(Ac_a^2 + B)}{2Bc_b(c_a^2 - 1)} \tag{31b}$$

where A and B are defined in (30a). Now, by setting a (with $c_b = a\cos\theta_{c1}$), parameters c_a and Z_{0_b} are defined precisely using (31). This means that, for a particular operating bandwidth, both the ripple value and the minimum rejection level are fixed. The computational complexity of (31) compared with (29) is similar. However, given a desired FBW by means of the general equations, it is possible to synthesize the filter with different ripple and rejection levels (see Fig. 10). Fig. 12 shows the S-parameters for the proposed filter having two bandwidths and several values of a, by using the general (29) with $L_R = [20, 30]$ dB and by means of the simplified expressions in (31) with $\bar{Z}_{0_a} = 1$. As can be seen, general design equations allow the value of L_R to be adjusted, but, when $\bar{Z}_{0_a} = 1$, the frequency response is automatically fixed for each value of a. Nevertheless, from these curves, it is noted that for values of L_R between 15 and 20 dB, the use of $Z_{0_a} = Z_0$ provides excellent results.

Furthermore, as shown in Fig. 8, the proposed topology can also be used to synthesize a three-pole quasi-elliptic filter. By imposing this condition on (24), the following equation has been derived:

$$\bar{Z}_{0_b}^2 + \frac{4\bar{Z}_{0_a}c_ac_b\left[\bar{Z}_{0_a}^2\left(c_a^2(2c_a^2-3)+c_b^2\right)+c_a^2(1-c_b^2)\right]}{4\left[\bar{Z}_{0_a}^2(c_b^2-c_a^2)+c_a^2(1-c_b^2)\right]^2}\bar{Z}_{0_b} + \frac{\bar{Z}_{0_a}^2c_a^2c_b^2\left(4\bar{Z}_{0_a}^2(c_a^2-1)+1\right)}{4\left[\bar{Z}_{0_a}^2(c_b^2-c_a^2)+c_a^2(1-c_b^2)\right]^2} = 0 \tag{32}$$

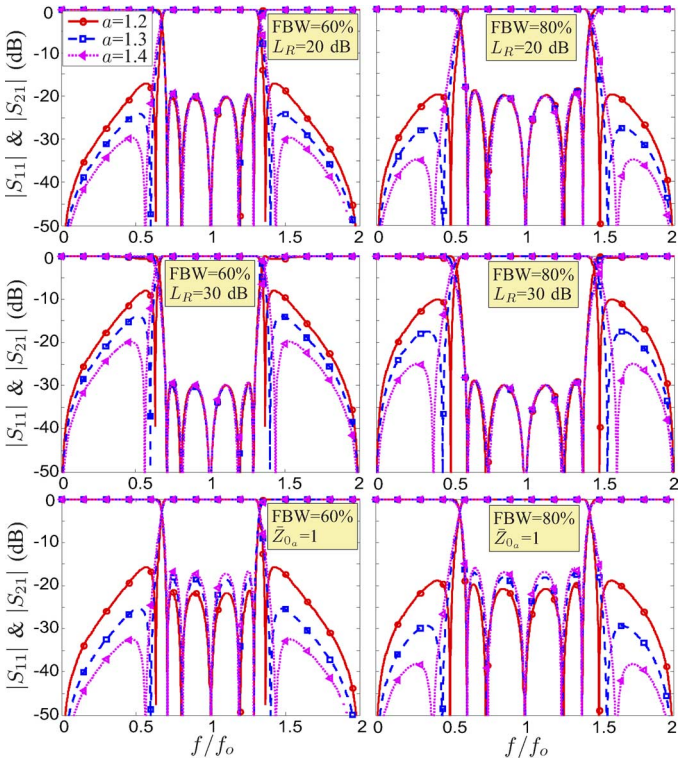

Fig. 12. Magnitude of S_{11} and S_{21} calculated using (29) with $L_R = [20, 30]$ dB and by using (31) with $\bar{Z}_{0_a} = 1$, for two operating fractional bandwidths FBW $= [60, 80]\%$ and several values of $a = [1.2, 1.3, 1.4]$.

where $\bar{Z}_{0_b}$ can be calculated by solving the quadratic equation as a function of c_a, c_b and $\bar{Z}_{0_a}$. Similar to the simplification for the general design expressions, if $\bar{Z}_{0_a} = 1$, then (32) reduces to

$$\bar{Z}_{0_b} = \frac{c_a\left(2c_a^2 - c_b^2 + 2\sqrt{c_a^4 - c_b^2c_a^2(1+c_b^2) + c_b^4}\right)}{2c_b^3\left(1 - c_a^2\right)}. \quad (33)$$

It is important to note that (32) and (33) establish a unique relationship between the series and shunt MTL, to obtain three poles within the passband, but unlike the general expressions for five poles, (29) or (31) ($\bar{Z}_{0_a} = 1$), there is no control on the required operating bandwidth. Therefore, some iteration is necessary before the desired performance can be achieved.

Finally, once the design parameters (c_a, Z_{0_a}, c_b, Z_{0_b}) for three- or five-pole quasi-elliptic bandpass filters have been calculated, the even- and odd-mode impedances for the series and shunt MTLs can be determined using the following expressions:

$$Z_{oe_i} = \frac{k_i - 1}{2} Z_{0_i}\,(R-1)\,\frac{1 - c_i^2}{c_i^2}$$

$$Z_{oo_i} = \frac{Z_{oe_i}}{R} \quad (34a)$$

$$R = \frac{c_i + \sqrt{(k_i-1)^2(1-c_i^2) + c_i^2}}{(k_i - 1)(1 - c_i)}. \quad (34b)$$

The above expression for (34) is derived from (4), (5), and (17)and provides the values for the even- and odd-mode impedances of both MTLs, as a function of k. The number of conductors (k) to achieve the required values of Z_{0_i} and c_i will depend

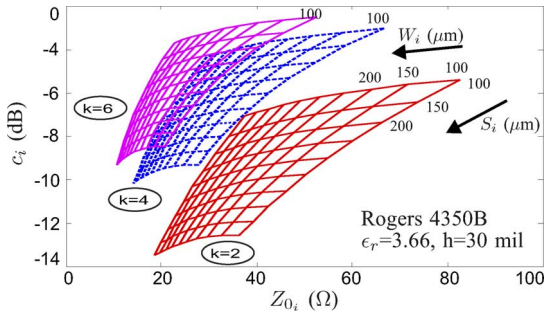

Fig. 13. Characteristic impedance Z_{0_i} (4) and coupling factor c_i (5) for the series and shunt wire-bonded MTL as a function of the number of conductors k, the line-width W and spacing S (grid spacing $=$ 50 μ m).

on the employed substrate and the manufacturing capabilities. In addition, it is important to note that the equations in (34) are different from the design equations for a k-line coupler [39]. In a four-port directional coupler, a condition for perfect match and perfect isolation ($Z_0^2 = 1/(M^2 - N^2)$) is imposed [39], but in this work the characteristic impedances of both MTLs (Z_{0_i}), c_a and c_b are calculated to achieve the desired frequency response. Here, c_a and c_b are design variables and may not be interpreted as the coupling factor of a directional coupler. In that sense, for example, the fabrication of a MTL with $c_i = -10$ dB can be more complicated than another with $c_i = -4$ dB, depending on its characteristic impedance Z_{0_i}. This behavior is illustrated in Fig. 13, where Z_{0_i} and c_i are represented as a function of the width W_i and spacing S_i for several numbers of conductors k. These curves have been calculated by using the Rogers 4350B substrate (having a dielectric constant of 3.66 and thickness of 30 mil). This substrate will be used throughout the rest of this work.

III. Experimental Validation

To validate our theory and techniques, several filters have been designed, fabricated and measured. Four five-pole and two three-pole quasi-elliptic filters are designed using the analytical equations (29a), (29b), and (32). Fig. 14 gives the predicted equation (24) and measured S-parameter results for the manufactured prototypes. The measured group delay responses and photographs of these filters are also shown in Fig. 14. The design center frequency was chosen to be $f_o = 3.5$ GHz. The physical dimensions and design parameters are given in Table III. The minimum allowed width and spacing dimensions are limited to 100 μ m, according to our in-house fabrication capability, which determines the range of achievable values of Z_{0_i} and c_i (see Fig. 13).

Fig. 14 shows agreement between the predicted and measured S-parameter results; it should be emphasized that there was no post-manufacture tuning. Three out of the four five-pole filters have been designed with an operating fractional bandwidth of 80% and the last one is designed with a bandwidth of 50%. For the three-pole filters, two operating bandwidths of 84% and 34% have been selected. It is important to highlight the excellent in-band flatness of the filters, with insertion losses below 1 dB in all the prototypes, and steep roll-off skirts. From Fig. 14(b) and (c), it can be seen that, given a desired FBW and a

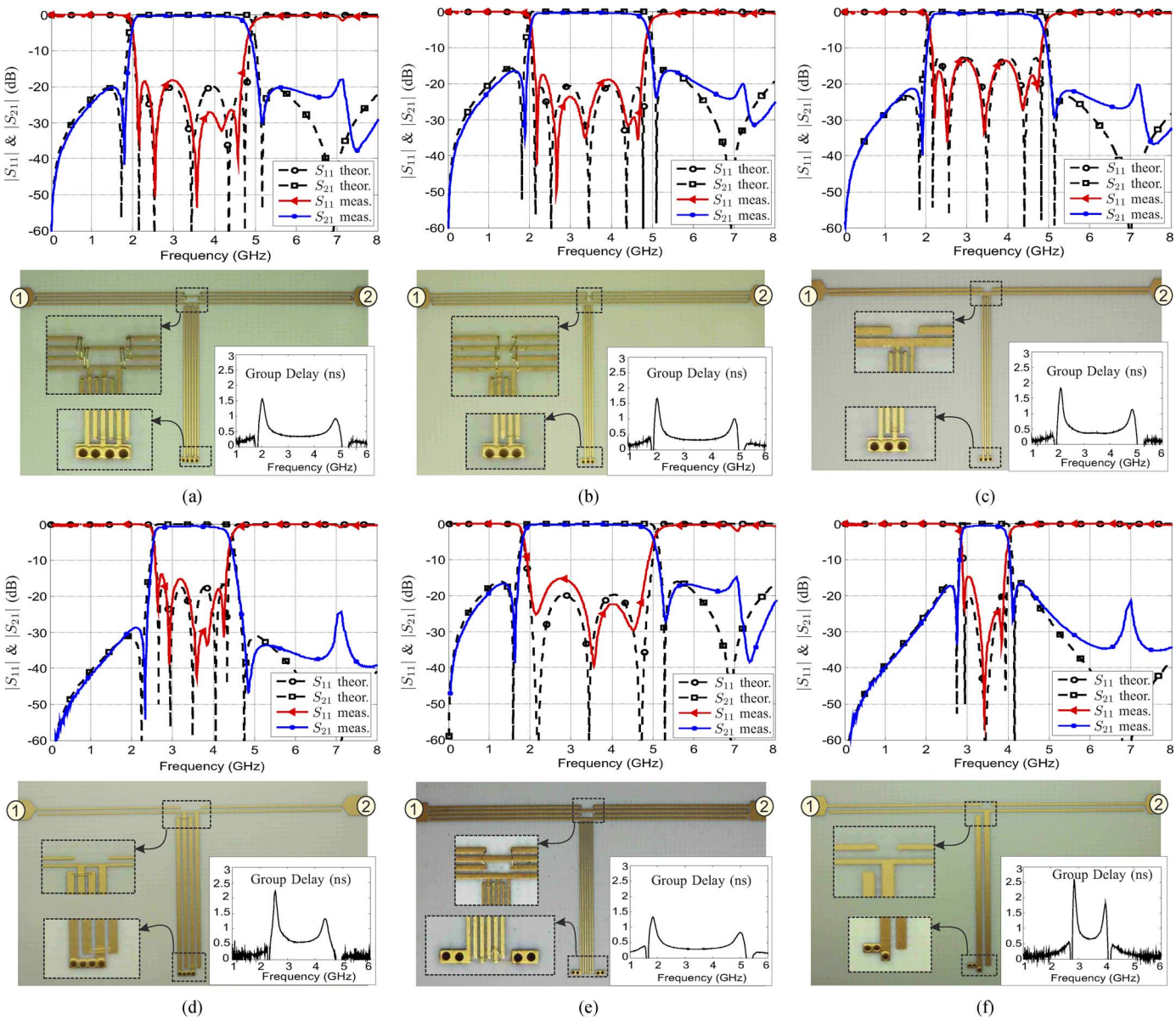

Fig. 14. Theoretical prediction (24) and measured S_{11}, S_{21} and group-delay parameter performances for the manufactured three- and five-pole quasi-elliptic filters (see Table III).

TABLE III
PHYSICAL DIMENSIONS OF THE FABRICATED FILTERS FOR A DESIGN CENTER FREQUENCY f_o = 3.5 GHz

	FBW (%)	a	Z_{0_a} (Ω)	Z_{0_b} (Ω)	c_a (dB)	c_b (dB)	Z_{oe_a} (Ω)	Z_{oo_a} (Ω)	Z_{oe_b} (Ω)	Z_{oo_b} (Ω)	k_a	W_a (μm)	S_a (μm)	k_b	W_b (μm)	S_b (μm)
Fig. 14(a)	80	1.22	50	48	-5.1	-2.9	217	92	223	74	4	100	230	6	114	125
Fig. 14(b)	80	1.17	50	65	-4.8	-3.1	219	90	235	72	4	100	215	4	100	105
Fig. 14(c)	80	1.17	60	65	-6.1	-3.1	180	59	235	72	2	230	100	4	100	105
Fig. 14(d)	50	1.4	52	30	-9.1	-5.4	203	96	140	62	2	115	290	4	375	200
Fig. 14(e)	84	1.21	50	52	-4	-2.5	198	72	236	71	4	160	150	6	100	100
Fig. 14(f)	34	1.3	40	32	-10.5	-10	174	93	128	66	2	170	390	2	430	300

FBW: Fractional bandwidth with equal-ripple response, ℓ_a=ℓ_b=13.5 mm

particular value of a, the rejection levels can be improved by increasing the value of Z_{O_a} but at the expense of worsening the return losses. In addition, all the filters exhibit sharp cutoff slopes ($a \leq 1.4$) and, as expected from theory, by increasing the value of a, it is possible to obtain higher rejection levels with good return losses [Fig. 14(d)]. Therefore, there is a tradeoff between selectivity, return losses and out of band rejection. Nevertheless, given an operating bandwidth, the attainable performance of the filter will be ultimately limited by the capability of the fabrication process.

Finally, it should be mentioned that the dimensions of the series and shunt MTL have been calculated theoretically [45], [46]and have not been optimized by any EM simulator. Discrepancies between the theory and measurements can be mainly attributed to material and fabrication tolerances, as well as unequal even- and odd-mode phase velocities in the MTLs. Because of this inequality, a spurious response can be seen at approximately twice the mid-band frequency ($2f_o = 7$ GHz). Fortunately, there are a number of different techniques (distributed and lumped-element compensation approaches), to equalize the phase velocity of both modes; beyond the scope of this work. Nevertheless, even without any optimization, the minimum rejection level is always better than 15 dB.

IV. Conclusion

A rigorous and comprehensive study of bandpass filters consisting of series input and output wire-bonded MTL with a shunt MTL has been presented. First, closed-form design equations have been derived for the design of both third-order Butterworth and Chebyshev responses by using two series MTL. From this, a new design procedure has been derived for the design of quasi-elliptic function filters, by introducing an additional shunt MTL. It has been shown that the new topology is suitable for synthesizing three- and five-pole quasi-elliptic filters with sharp cutoff slopes. To demonstrate the validity and accuracy of the proposed analytical design equations, several prototypes have been designed, fabricated and measured. All of the prototypes exhibited low insertion losses (< 1 dB) with enhanced roll-off characteristic at both the lower and upper cutoff frequencies. In addition, the excellent agreement between the theoretical predictions and measured results should give designers the confidence to use the theory given in this work for a fast and accurate synthesis of bandpass filters for a desired frequency response.

References

[1] J.-S. Hong, *Microstrip Filters for RF/Microwave Applications*, K. Chang, Ed. New York, NY, USA: Wiley-Interscience, 2011.

[2] Z.-C. Hao and J.-S. Hong, "Ultrawideband filter technologies," *IEEE Microw. Mag.*, vol. 11, no. 4, pp. 56–68, Jun. 2010.

[3] G. L. Mattahei, L. Young, and E. M. T. Jones, *Microwave Filters, Impedance-Matching Networks, and Coupling Structures*, M. A. House, Ed. Norwood, MA, USA: Artech House, 1985.

[4] I. C. Hunter, *Theory and Design of Microwave Filters*, Stevenage, Ed. London, U.K.: Inst. Electr. Eng., 2001.

[5] X. Huang and S. Lucyszyn, "Silicon RFIC UWB bandpass filter using bulk-micromachined trench couplers," in *Proc. IEEE Int. . Wireless Symp.*, Beijing, China, Apr. 2013.

[6] W. Menzel, L. Zhu, K. Wu, and F. Bogelsack, "On the design of novel compact broad-band planar filters," *IEEE Trans. Microw. Theory Techn.*, vol. 51, no. 2, pp. 364–370, Feb. 2003.

[7] L. Zhu, S. Sun, and W. Menzel, "Ultra-wideband (UWB) bandpass filters using multiple-mode resonator," *IEEE Microw. Wireless Compon. Lett.*, vol. 15, no. 11, pp. 796–798, Nov. 2005.

[8] P. Cai, Z. Ma, X. Guan, Y. Kobayashi, T. Anada, and G. Hagiwara, "Synthesis and realization of novel ultra-wideband bandpass filters using 3/4 wavelength parallel-coupled line resonators," in *Proc. Asia–Pacific Microw. Conf.*, Dec. 2006, pp. 159–162.

[9] P. Cai, Z. Ma, X. Guan, T. Anada, and G. Hagiwara, "Synthesys and realization of ultra-wideband bandpass filters using the z-transform techinque," *Microw. Opt. Technol. Let.*, vol. 48, no. 7, pp. 1398–1401, Jul. 2006.

[10] C.-P. Chen, Z. Ma, and T. Anada, "Synthesis of ultra-wideband bandpass filter employing parallel-coupled stepped-impedance resonators," *IET Microw. Antennas Propag.*, vol. 2, no. 8, pp. 766–772, Dec. 2008.

[11] R. Li, S. Sun, and L. Zhu, "Synthesis design of ultra-wideband bandpass filters with composite series and shunt stubs," *IEEE Microw. Wireless Compon. Lett.*, vol. 57, no. 3, pp. 684–692, Mar. 2009.

[12] S. Sun, R. Li, L. Zhu, and W. Menzel, "Studies on synthesis design of ultra-wideband parallel-coupled line bandpass filters with Chebyshev responses," in *Proc. Asia–Pacific Microw. Conf.*, Dec. 2009, pp. 155–158.

[13] R. Zhang and L. Zhu, "Synthesis design of a wideband bandpass filter with inductively coupled short-circuited multi-mode resonator," *IEEE Trans. Microw. Theory Techn.*, vol. 22, no. 10, pp. 509–511, Oct. 2012.

[14] Y.-C. Chiou, J.-T. Kuo, and E. Cheng, "Broadband quasi-Chebyshev bandpass filters with multimode stepped-impedance resonators (SIRs)," *IEEE Trans. Microw. Theory Techn.*, vol. 54, no. 8, pp. 3352–3358, Aug. 2006.

[15] S. Sun and L. Zhu, "Multiple-resonator-based bandpass filters," *IEEE Microw. Mag.*, vol. 10, no. 2, pp. 88–98, Apr. 2009.

[16] S. W. Wong and L. Zhu, "Quadruple-mode UWB bandpass filter with improved out-of-band rejection," *IEEE Microw. Wireless Compon. Lett.*, vol. 19, no. 3, pp. 152–154, Mar. 2009.

[17] T. H. Duong and I. S. Kim, "New elliptic function type UWB BPF based on capacitively coupled $\lambda/4$ open T resonator," *IEEE Trans. Microw. Theory Techn.*, vol. 57, no. 12, pp. 3089–3098, 2009.

[18] L. Han, K. Wu, and X. Zhang, "Development of packaged ultra-wideband bandpass filters," *IEEE Trans. Microw. Theory Techn.*, vol. 58, no. 1, pp. 220–228, Jan. 2010.

[19] Y. Omote, T. Yasuzumi, T. Uwano, and O. Hashimoto, "Design procedure of wideband band-pass filter consists of inter-digital finger resonator and parallel coupled lines," in *Proc. Asia–Pacific Microw. Conf.*, Dec. 2010, pp. 29–32.

[20] X. Luo, J.-G. Ma, and E.-P. Li, "Wideband bandpass filter with wide stopband using loaded BCMC stub and short-stub," *IEEE Microw. Wireless Compon. Lett.*, vol. 21, no. 7, pp. 353–355, Jul. 2011.

[21] Q.-X. Chu, X.-H. Wu, and X.-K. Tian, "Novel UWB bandpass filter using stub-loaded multiple-mode resonator," *IEEE Microw. Wireless Compon. Lett.*, vol. 21, no. 8, pp. 403–405, Aug. 2011.

[22] H. Shaman, "New S-band bandpass filter (BPF) with wideband passband for wireless communication systems," *IEEE Microw. Wireless Compon. Lett.*, vol. 22, no. 5, pp. 242–244, May 2012.

[23] C.-P. Chen, J. Oda, T. Anada, Z. Ma, and S. Takeda, "Theoretical design of wideband filters with attenuation poles using improved parallel-coupled three-line units," in *IEEE MTT-S Int. Microw. Symp. Dig.*, Jun. 2012, pp. 1–3.

[24] H. Zhu and Q.-X. Chu, "Compact Ultra-Wideband (UWB) bandpass filter using Dual-Stub-Loaded Resonator (DSLR)," *IEEE Microw. Wireless Compon. Lett.*, vol. 23, no. 10, pp. 527–529, 2013.

[25] S. Khalid, P. W. Wong, and L. Y. Cheong, "A novel synthesis procedure for ultra wideband (UWB) bandpass filters," *Progr. Electromagn. Res.*, vol. 141, pp. 249–266, 2013.

[26] J. J. Sánchez-Martínez, E. Márquez-Segura, and S. Lucyszyn, "Design of compact wideband bandpass filters based on multiconductor transmission lines with interconnected alternate lines," *IEEE Microw. Wireless Compon. Lett.*, vol. 24, no. 7, pp. 454–456, Jul. 2014.

[27] W.-T. Wong, Y.-S. Lin, C.-H. Wang, and C. H. Chen, "Highly selective microstrip bandpass filters for ultra-wideband (UWB) applications," in *Proc. Asia–Pacific Microw. Conf.*, Dec. 2005, vol. 5.

[28] H. Shaman and J.-S. Hong, "Input and output cross-coupled wideband bandpass filter," *IEEE Trans. Microw. Theory Techn.*, vol. 55, no. 12, pp. 2562–2568, Dec. 2007.

[29] S. Sun and L. Zhu, "Wideband microstrip ring resonator bandpass filters under multiple resonances," *IEEE Trans. Microw. Theory Techn.*, vol. 55, no. 10, pp. 2176–2182, Oct. 2007.

[30] J.-Y. Li, C.-H. Chi, and C.-Y. Chang, "Synthesis and design of generalized Chebyshev wideband hybrid ring based bandpass filters with a controllable transmission zero pair," *IEEE Trans. Microw. Theory Techn.*, vol. 58, no. 12, pp. 3720–3731, Dec. 2010.

[31] W. J. Feng, W. Q. Che, Y. M. Chang, S. Y. Shi, and Q. Xue, "High selectivity fifth-order wideband bandpass filters with multiple transmission zeros based on transversal signal-interaction concepts," *IEEE Trans. Microw. Theory Techn.*, vol. 61, no. 1, pp. 89–97, Jan. 2013.

[32] A. Abbosh, "Design method for ultra-wideband bandpass filter with wide stopband using parallel-coupled microstrip lines," *IEEE Trans. Microw. Theory Techn.*, vol. 60, no. 1, pp. 31–38, Jan. 2012.

[33] S. Amari, F. Seyfert, and M. Bekheit, "Theory of coupled resonator microwave bandpass filters of arbitrary bandwidth," *IEEE Trans. Microw. Theory Techn.*, vol. 58, no. 8, pp. 2188–2203, Aug. 2010.

[34] W. Meng, H.-M. Lee, K. Zaki, and A. Atia, "Synthesis of wideband multicoupled resonators filters," *IEEE Trans. Microw. Theory Techn.*, vol. 59, no. 3, pp. 593–603, Mar. 2011.
[35] R. Mongia, I. Bahl, and P. Bhartia, *RF and Microwave Coupled-Line Circuits*. Norwood, MA, USA: Artech House, 1999.
[36] E. Márquez-Segura, F. Casares-Miranda, P. Otero, C. Camacho-Peñalosa, and J. Page, "Analytical model of the wire-bonded interdigital capacitor," *IEEE Trans. Microw. Theory Techn.*, vol. 54, no. 2, pp. 748–754, Feb. 2006.
[37] J. J. Sánchez-Martínez and E. Márquez-Segura, "Generalized analytical design of broadband planar baluns based on wire-bonded multiconductor transmission lines," *Progr. Electromagn. Res.*, vol. 134, pp. 169–187, 2013.
[38] J. J. Sánchez-Martínez and E. Márquez-Segura, "Analysis of wire-bonded multiconductor transmission line-based phase-shifting sections," *J. Electromagn. Waves Appl.*, vol. 27, no. 16, pp. 1997–2009, Sep. 2013.
[39] W. Ou, "Design equations for an interdigitated directional coupler," *IEEE Trans. Microw. Theory Techn.*, vol. MTT-23, no. 2, pp. 253–255, Feb. 1975.
[40] J. J. Sánchez-Martínez, E. Márquez-Segura, and C. Camacho-Peñalosa, "Synthesis of CRLH-TLs based on a shunt coupled-line section," in *Proc. 42nd Eur. Microw. Conf.*, Oct. 2012, pp. 675–678.
[41] H.-R. Ahn and T. Itoh, "Impedance-transforming symmetric and asymmetric DC blocks," *IEEE Trans. Microw. Theory Techn.*, vol. 58, no. 9, pp. 2463–2474, Sep. 2010.
[42] M. Abramowitz and I. Stegun, *Handbook of Mathematical Functions With Formulas, Graphs, and Mathematical Tables*. Washington, DC, USA: U.S. Gov. Printing Office, 1972.
[43] J. J. Sánchez-Martínez, E. Márquez-Segura, and C. Camacho-Peñalosa, "Analysis of wire-bonded multiconductor transmission-line-based stubs," *IEEE Trans. Microw. Theory Techn.*, vol. 61, no. 4, pp. 1467–1476, Apr. 2013.
[44] R. Levy, "Filters with single transmission zeros at real or imaginary frequencies," *IEEE Trans. Microw. Theory Techn.*, vol. 24, no. 4, pp. 172–181, Apr. 1976.
[45] M. Kirschning and R. Jansen, "Accurate wide-range design equations for the frequency-dependent characteristic of parallel coupled microstrip lines," *IEEE Trans. Microw. Theory Techn.*, vol. 32, no. 1, pp. 83–90, Jan. 1984.
[46] J. A. B. Faria, "Kirschning and Jansen computer-aided design formulae for the analysis of parallel coupled lines," *Microw. Opt. Technol. Let.*, vol. 51, no. 10, pp. 2466–2470, 2009.

Juan José Sánchez-Martínez received the B.S., M.S., and Ph.D. degrees in telecommunication engineering from the University of Málaga, Málaga, Spain, in 2003, 2006, and 2014, respectively.

Since March 2006, he has been a Research Assistant with the Department of Communication Engineering, University of Málaga, Málaga, Spain. He was involved with signal processing for digital communications and real-time implementation of signal processing algorithms on field-programmable gate array until 2010. From May to August 2012, he was a Visiting Scholar with the Department of Electrical and Electronic Engineering, Imperial College London, London, U.K. His current research is focused on the analysis of planar structures and the design of microwave passive devices.

Mr. Sánchez-Martínez was the recipient of a Junta de Andalucía Scholarship (2010–2014).

Enrique Márquez-Segura (S'93–M'95–SM'06) was born in Málaga, Spain, in April 1970. He received the Ingeniero de Telecomunicación and Doctor Ingeniero degrees from the Universidad de Málaga, Málaga, Spain, in 1993 and 1998, respectively.

In 1994, he joined the Departamento de Ingeniería de Comunicaciones, Escuela Técnica Superior de Ingeniería (ETSI) de Telecomunicación, Universidad de Málaga, Málaga, Spain, where, in 2001, he became an Associate Professor. His current research interests include electromagnetic material characterization, measurement techniques, and RF and microwave circuits design for communication applications.

Dr. Márquez-Segura was the recipient of a Spanish Ministry of Education and Science Scholarship (1994–1995).

Stepan Lucyszyn (M'91–SM'04–F'14) received the Ph.D. degree in electronic engineering from King's College London, University of London, London, U.K., in 1992, and the D.Sc. degree in millimeter-wave and terahertz electronics from Imperial College London, London, U.K., in 2010.

He is currently a Reader (Associate Professor) in millimeter-wave electronics and Director of the Centre for Terahertz Science and Engineering, Imperial College London. After working in industry as a Satellite Systems Engineer for maritime and military communications, he spent the first 12 years researching microwave and millimeter-wave RF integrated circuits (RFICs)/monolithic microwave integrated circuits (MMICs), followed by RF microelectromechanical systems (MEMS) technologies. For over 17 years, he has been involved with millimeter-wave electronics, and since 2004, with the investigation of the behavior of materials, passive structures, and ubiquitous applications at terahertz frequencies. For the past 16 years, he has taught MMIC measurement techniques at the National Physical Laboratory (NPL), Teddington, Middlesex, U.K. He has coauthored approximately 170 papers and 12 book chapters in applied physics and electronic engineering. He has delivered many invited presentations at international conferences.

Dr. Lucyszyn is a Fellow of the Institution of Electrical Engineers (U.K.), the Institute of Physics (U.K.), and the Electromagnetics Academy. He was an associate editor for the IEEE JOURNAL OF MICROELECTROMECHANICAL SYSTEMS (2005 to 2009). In 2011, he was the chairman of the 41st European Microwave Conference, Manchester, U.K. In 2009, he was appointed an IEEE Distinguished Microwave Lecturer (DML) (2010–2012) and Emeritus DML (2013). He is currently a European Microwave Lecturer (EML) for the European Microwave Association.